Metabolic Theory and the Temperature-Size Rule Explain the Temperature Dependence of Population Carrying Capacity

Article *in* The American Naturalist · October 2018

DOI: 10.1086/700114

CITATIONS
19

READS
739

3 authors, including:

Joey R. Bernhardt
University of British Columbia - Vancouver
39 PUBLICATIONS **1,509** CITATIONS

SEE PROFILE

Mary I. O'Connor
University of British Columbia - Vancouver
65 PUBLICATIONS **5,365** CITATIONS

SEE PROFILE

Metabolic Theory and the Temperature-Size Rule Explain the Temperature Dependence of Population Carrying Capacity

Joey R. Bernhardt,[1,*] Jennifer M. Sunday,[1,2] and Mary I. O'Connor[1]

1. Department of Zoology, Biodiversity Research Centre, University of British Columbia, Vancouver, British Columbia V6T 1Z4, Canada; 2. School of Marine and Environmental Affairs, University of Washington, Seattle, Washington 98195

Submitted October 29, 2017; Accepted June 7, 2018; Electronically published October 22, 2018

Online enhancements: appendix. *Dryad data:* https://doi.org/10.5061/dryad.9kv23s3.

ABSTRACT: The temperature dependence of highly conserved subcellular metabolic systems affects ecological patterns and processes across scales, from organisms to ecosystems. Population density at carrying capacity plays an important role in evolutionary processes, biodiversity, and ecosystem function, yet how it varies with temperature-dependent metabolism remains unclear. Though the exponential effect of temperature on intrinsic population growth rate, r, is well known, we still lack clear evidence that population density at carrying capacity, K, declines with increasing per capita metabolic rate, as predicted by the metabolic theory of ecology (MTE). We experimentally tested whether temperature effects on photosynthesis propagate directly to population carrying capacity in a model species, the mobile phytoplankton *Tetraselmis tetrahele*. After maintaining populations at a fixed resource supply and fixed temperatures for 43 days, we found that carrying capacity declined with increasing temperature. This decline was predicted quantitatively when models included temperature-dependent metabolic rates and temperature-associated body-size shifts. Our results demonstrate that warming reduces carrying capacity and that temperature effects on body size and metabolic rate interact to determine how temperature affects population dynamics. These findings bolster efforts to relate metabolic temperature dependence to population and ecosystem patterns via MTE.

Keywords: metabolic scaling theory, photosynthesis, metabolism, temperature, carrying capacity, body size.

Introduction

At ecosystem scales, patterns of species abundance and fluxes of energy and materials reflect the summed performance of individual organisms. Organismal metabolic performance is sensitive to temperature in a manner that explains substantial variation in ecosystem processes along temperature gradients (López-Urrutia et al. 2006; Anderson-Teixeira et al. 2008; Yvon-Durocher et al. 2012). In these examples from marine, freshwater, and terrestrial systems, the temperature dependence of highly conserved metabolic rates (e.g., photosynthesis and aerobic respiration) emerges at community and ecosystem scales, even when temperature also affects population dynamics and species interactions within these ecosystems. Understanding how temperature-dependent metabolism modifies population dynamics and ultimately affects community and ecosystem processes is a current challenge in an ecological science striving for unified understanding across scales and levels of organization.

Density of a population at carrying capacity is a key concept linking population dynamics to broader-scale patterns of biodiversity and population persistence (Damuth 1987; Savage et al. 2004; Allen et al. 2007; O'Gorman et al. 2017; Uszko et al. 2017). Carrying capacity refers to the abundance of a population under steady-state conditions. Though it is a parameter in the simplest logistic growth models, it is understood to be an emergent property that reflects density-dependent birth and death rates (Mallet 2012; Doebeli et al. 2017; Uszko et al. 2017) or relative growth and loss rates (McCann 2011; Gilbert et al. 2014) that balance to maintain steady population density through time. Density-dependent birth and death rates limit population growth rate at densities far below carrying capacity, at all but very low densities. As a theoretical attribute of populations growing in an environment with limited resources, density at carrying capacity is as important as intrinsic growth rate to understanding population dynamics (Gotelli 1995; Gilbert et al. 2014; Uszko et al. 2017).

Efforts to scale up from how temperature affects individual performance to the outcomes of population, community, and ecosystem processes must assume a relationship between temperature and population carrying capacity (Savage et al. 2004; Allen et al. 2005, 2007; O'Connor et al. 2011; Gilbert et al. 2014; O'Gorman et al. 2017). The metabolic theory of ecology (MTE) postulates that the temperature dependence of widely shared metabolic rates (photosynthesis and respiration) drives temperature dependence of demographic

* Corresponding author; email: joey.bernhardt@biodiversity.ubc.ca.
ORCIDs: Bernhardt, http://orcid.org/0000-0003-1824-2801; O'Connor, http://orcid.org/0000-0001-9583-1592.

Am. Nat. 2018. Vol. 192, pp. 000–000.
DOI: 10.1086/700114

rates (birth, death), leading to predictable effects of temperature on population growth (Savage et al. 2004; López-Urrutia et al. 2006; López-Urrutia 2008; Kremer et al. 2017) and community-level patterns (Savage et al. 2004; Allen et al. 2005, 2007; Meehan 2006; Osmond et al. 2017; Sentis et al. 2017). Savage et al. (2004) reasoned that carrying capacity would be expected to decline exponentially, with increasing temperature reflecting exponential temperature-induced increases in per capita metabolic resource demand, driven by exponential increases in per capita respiration rate. Subsequent models linking temperature-dependent metabolism to population- and community-level processes such as relative biomass across trophic levels have adopted this assumption (Allen et al. 2007; O'Connor et al. 2011; Gilbert et al. 2014; O'Gorman et al. 2017), while other studies have assumed no relationship between temperature and carrying capacity (Vasseur and McCann 2005; Sentis et al. 2017). Temperature-dependent consumer-resource models have shown how the assumed temperature dependence of carrying capacity of primary producers modulates food-web responses to warming (O'Connor et al. 2011; Gilbert et al. 2014; O'Gorman et al. 2017; Osmond et al. 2017), although concomitant increases in nutrient supply with warming can buffer responses to temperature by reducing resource limitation (O'Connor et al. 2011; Gilbert et al. 2014; O'Gorman et al. 2017). If the effect of temperature on carrying capacity is general under constant resource conditions, it could be extended to estimates of ecosystem-level processes such as the productivity of marine fisheries (Pauly and Christensen 1995; Sarker and Wiltshire 2017), geographic range-expansion rates (Fronhofer and Altermatt 2015), or rates and direction of evolutionary change (Mallet 2012; Hendry 2017).

First-order MTE models and population dynamic models that relate per capita metabolic rate to density at carrying capacity have assumed that body size and other traits that could influence carrying capacity do not covary with temperature (Savage et al. 2004; O'Connor et al. 2011; Gilbert et al. 2014). However, this assumption contradicts substantial evidence that body size changes with temperature (Atkinson et al. 2003; Forster et al. 2012). Declines in body size of 1.7%–3.3% $°C^{-1}$ (cell size in unicellular organisms) are widely observed responses to warming that can arise due to phenotypic plasticity or selection for smaller body sizes (Atkinson et al. 2003; DeLong 2012; Forster et al. 2012). This decline in body size is called the temperature-size rule (TSR) and can mediate population dynamic responses to warming in the presence of consumers (Osmond et al. 2017). Warming-induced body-size declines could alter predictions of population density over a temperature gradient if smaller individual sizes alleviate resource limitation and allow greater population densities than would be predicted for larger individuals.

We hypothesized that the temperature dependence of per capita metabolic rates accurately predicts the decline in density at carrying capacity with increasing temperature within a population's range of suboptimal temperatures (Savage et al. 2004). To test this hypothesis, we maintained populations of the marine phytoplankton *Tetraselmis tetrahele* for 43 days over an experimental temperature gradient spanning 5°–38°C and estimated their per capita oxygen consumption and production rates, mean cell size, intrinsic population growth rate (r), and steady-state abundance (K). We expected cell size to decline with increasing temperature, and we tested the alternate hypothesis that declines in cell size would mitigate declines in density at carrying capacity with increasing temperature. This is, to our knowledge, the first experimental test of hypotheses that explicitly contrast predictions based on the temperature dependence of metabolic rates and the TSR under carefully controlled resource conditions that meet the assumptions of the logistic growth model. We found that changes in metabolic rate and body size can together be used to quantitatively predict declines in carrying capacity with temperature according to the MTE, and we used these results to modify an existing general modeling framework (Savage et al. 2004) for how temperature-dependent metabolism scales to population dynamics. Our experiment provides novel empirical support for an often-made theoretical assumption in general population models about how temperature affects carrying capacity.

Methods

We modeled the effects of temperature on logistic population growth in terms of the temperature dependence of highly conserved metabolic rates (photosynthesis and aerobic respiration). We used the logistic model because it has been widely used to link the general body size and temperature dependence of metabolism to population and ecosystem patterns (Savage et al. 2004; Gilbert et al. 2014; O'Gorman et al. 2017). In the logistic growth model

$$\frac{dN}{dt} = rN\left(1 - \frac{N}{K}\right), \tag{1}$$

N is the size of the population at time t, r is the intrinsic growth rate, and carrying capacity K is the value of $N > 0$ that makes $dN/dt = 0$ (Verhulst 1838; Gotelli 1995).

Savage et al. (2004) applied the metabolic theory of ecology to relate logistic growth to the temperature dependence of metabolic rate by assuming that allocation of metabolic resources to new individuals (vs. to somatic growth or maintenance) is independent of temperature. Population-level resource use is set by the total metabolic rate of the population (B_{pop}), which is equal to the average individual metabolic rate (B_i) summed over all individuals in the population. Carrying capacity occurs when the rate of resource use by the population equals the rate of resource supply to the population (P), such that $B_{pop} = P$. The number of individuals at

carrying capacity K is limited by average individual metabolic rate

$$K(M_i, T) \propto \frac{B_{\text{pop}}}{B_i(M_i, T)}, \tag{2}$$

where $B_i(M_i, T)$ is the average individual metabolic rate at steady state, which varies with average individual body size (M_i) and temperature (T, in Kelvin). Metabolic rate B_i scales with body mass and increases with temperature:

$$B_i(M_i, T) = b_{0i} M_i^{3/4} e^{-E_a/kT}, \tag{3}$$

where b_{0i} is a normalization constant, E_a is the activation energy of metabolism (Gillooly et al. 2001), k is Boltzmann's constant, and T is temperature in Kelvin. Equation (2) shows that an increase in individual metabolic rate will lead to a decrease in density, $K(M_i, T)$, for a population at steady state ($B_{\text{pop}} = P$) with a constant, temperature-independent resource supply, P. Combining equations (2) and (3) shows how $K(M_i, T)$ is predicted to scale directly with mass- and temperature-dependent metabolic rate:

$$K(M_i, T) \propto M_i^{-3/4} e^{E_a/kT}. \tag{4}$$

From here, we depart from previous models (Savage et al. 2004; O'Connor et al. 2011) and allow body size, M_i, to decline linearly with increasing temperature (consistent with the TSR in ectotherms):

$$M_i(T) = M_i^{T_R}[1 - \beta(T - T_R)], \tag{5}$$

where β is the fraction by which body mass is reduced as temperature T is increased by 1°C, T_R is a reference temperature, and $M_i^{T_R}$ is average mass at T_R (Osmond et al. 2017). This linear approximation of the TSR is appropriate for unicellular organisms (Atkinson et al. 2003; DeLong 2012; Forster et al. 2012). We can express our hypothesis that temperature-induced changes in size and temperature-dependent per capita metabolic rate both determine how carrying capacity depends on temperature by substituting the temperature-dependent body-size model (eq. [5]) into the equation for the temperature dependence of K (eq. [4]):

$$K(M_i, T) \propto (M_i^{T_R}[1 - \beta(T - T_R)])^{-3/4} e^{E_a/kT}. \tag{6}$$

When mass is independent of temperature ($\beta = 0$), the temperature dependence of K is entirely captured by the temperature dependence of metabolism (E_a). However, decreases in body size with temperature ($\beta > 0$) will reduce temperature-induced declines in K.

To linearize equation (6) for comparison with experimental results, we first collapsed the temperature-dependent mass term to $M_i(T)^{-3/4}$, rearranged terms, and then took the natural log of both sides:

$$\ln(KM_i(T)^{3/4}) \propto \frac{E_a}{kT}. \tag{7}$$

A critical test of the hypothesis that changes in carrying capacity can be predicted from the temperature dependence of metabolism and body size would be to test that the association between $\ln(KM_i(T)^{3/4})$ and temperature, in units of $1/kT$, yields a slope that is equal to E_a. We tested this hypothesis experimentally with a photosynthetic autotroph, and we used $E_a = E_{GP}$, where E_{GP} is the activation energy of gross photosynthesis (Brown et al. 2004; Gilbert et al. 2014; Padfield et al. 2016; O'Gorman et al. 2017). Gross photosynthesis (GP) is the total carbon fixed through photosynthesis, from which some portion is respired in the conversion of fixed carbon to biomass (somatic growth or reproduction). We used an Arrhenius function to describe the temperature dependence of metabolic rate (GP) for temperatures up to the estimated thermal optimum (25°C; fig. A1; figs. A1–A8 are available online) and constrained our analysis to the increasing portion of the thermal performance curve (Pawar et al. 2016). We focused on a range of suboptimal temperatures because biological rates decline sharply with increases in temperature beyond the thermal optimum. To model the full thermal response curve, a unimodal function such as the Sharpe-Schoolfield equation is often used (Schoolfield et al. 1981). Also, focusing on the relationship between temperature and population parameters over the range of suboptimal temperatures is appropriate for scaling from individual metabolic responses to temperature to broader community and ecosystem scales (Savage et al. 2004; Yvon-Durocher and Allen 2012). When a population's abundance approaches 0 due to thermal stress, another species with a different thermal niche is likely to be present and abundant, compensating for the functions performed by the population declining due to stress (Yvon-Durocher et al. 2012; Padfield et al. 2017).

We used the temperature dependence of GP and body size in equation (7) to predict how temperature-dependent metabolic rate limits population growth rate and carrying capacity (table 1). Our purpose was to test this prediction empirically under controlled conditions for a single population with independent measures of oxygen metabolism and population dynamics. We tested the model assumption that energy allocation remains constant over a thermal gradient by estimating the temperature dependence of the ratio of gross photosynthesis to respiration (GP/R). We predicted that in the absence of systematic changes in body size with temperature, the temperature dependence of K would be inversely proportional to the temperature dependence of GP, $E_{K,N} = -E_{GP}$ (here we use the subscript K, N to refer to K estimated in terms of number of individuals, to distinguish it from K es-

Table 1: Temperature dependences of per capita metabolic rates, body size, and population carrying capacity estimated from experimental populations of *Tetraselmis tetrahele* grown over a temperature gradient from 5° to 25°C

Parameter	Predicted temperature dependence	Estimate	95% CI	Regression model with fitted fixed coefficients
1. E_{GP}	.32 eV[a,b,c]	.33 eV	.20, .46	$\ln(GP \times M_i^{-3/4}) = 1.28 - .33(1/kT)$
2. E_{NP}	.32 eV[a,b,c]	.24 eV	−.02, .51	$\ln(NP \times M_i^{-3/4}) = -3.24 - .24(1/kT)$
3. E_R	.65 eV[d]	.52 eV	.39, .66	$\ln(R \times M_i^{-3/4}) = 8.48 - .52(1/kT)$
4. $E_{K,N}$	−.32 eV[e]	−.22 eV	−.25, −.18	$\ln(K_N \times M_i^{-3/4}) = 4.22 + .22(1/kT)$
5. $E_{K,N}$	−.32 eV[e]	−.34 eV	−.37, −.31	$\ln(K_N \times M_i(T)^{3/4}) = -.84 + .34(1/kT)$
6. $E_{K,Bio}$	−.32 eV[e]	−.30 eV	−.33, −.26	$\ln(K_{Bio}) = 2.37 + .30(1/kT)$
7. β	2.5%°C^{-1}[f]	1.92%°C^{-1}	1.48%, 2.36%	$M_i(T) = 81.87[1 - \beta (T - 5)]$; $\beta = .00192$

Note: Parameters 4 and 5 refer to the temperature dependence of carrying capacity estimated two ways: with a temperature-independent body mass (4) and with a temperature-dependent body mass (5). CI = confidence interval. References are as follows:

[a] Allen et al. 2005.

[b] Yvon-Durocher and Allen 2012.

[c] López-Urrutia et al. 2006.

[d] Gillooly et al. 2001.

[e] Savage et al. 2004.

[f] Atkinson et al. 2003.

timated in terms of biomass, which we will do later). If, however, body size declines as predicted by the temperature-size rule, then the observed decline in K with temperature would be less than expected based on temperature-dependent photosynthesis. In contrast, a plot of mass-normalized $\ln(KM_i(T)^{3/4})$ against $1/kT$ will yield a slope equal to $-E_{GP}$ if K is estimated in terms of biomass, K_{Bio}. Here K_{Bio} combines cell size and cell density, and so $\ln(K_{Bio})$ plotted against $1/kT$ should decline with a slope equal to $-E_{GP}$.

Study System

We tested our hypotheses in a closed phytoplankton microcosm system with fixed energy and nutrient supplies. We used the flagellated marine chlorophyte *Tetraselmis tetrahele*, a globally distributed coastal marine phytoplankton species. *Tetraselmis tetrahele* is eurythermal, meaning populations are found at a broad range of temperatures below its thermal optimum around 25°C. It is an important photosynthetic food source in nearshore food webs with a generation time of ~1 day at 20°C (Pena and Villegas 2005), making it a suitable species for microcosm studies and tests of metabolic scaling theory. The high mobility of this plankton species suggests that individuals can gain equal access to resources by moving throughout the microcosm, making it a good model species for meeting the assumptions underlying our hypotheses (eq. [7]). We used a cultured strain obtained from the Canadian Centre for the Culture of Microorganisms (UW414), originally isolated off the coast of Vancouver Island, British Columbia. *Tetraselmis tetrahele* were maintained in laboratory culture in ESAW (enriched seawater, artificial water) medium (Harrison et al. 1980) in 30-mL glass test tubes at 16°C for 1 year on a 16L : 8D photoperiod under nutrient- and light-saturated conditions before the start of the experiments.

Experimental Conditions

We set carrying capacity based on nitrate availability in experimental cultures. Though algal growth models have shown that nutrient and light limitation can have slightly different effects on equilibrium abundance and dynamics (Thomas et al. 2017; Uszko et al. 2017), we chose to limit one resource (nitrogen) to avoid potential complications associated with multiple limiting resources. We reduced the nitrate concentration by 55-fold relative to complete ESAW medium (final concentration 10 μM) to ensure that nitrate concentration limited population densities. In pilot experiments, we confirmed nitrate limitation by comparing to cell densities at steady state when grown at higher nitrate levels and by observing no increase in abundance at higher light levels. To assess how population-level nitrate use at carrying capacity changes with temperature, we measured nitrate remaining in experimental microcosm water columns at steady state. At the end of the experiment, we filtered 2 mL of experimental medium containing well-mixed phytoplankton onto GF/F filters. We assayed nitrate concentrations spectrophotometrically from the filtrate using a cadmium reduction method (Strickland and Parsons 1968; LaMotte Nitrate Nitrogen Test Kit) with a Turner Designs Trilogy fluorometer (nitrate/nitrite module 7200-074).

Sampling Cell Density and Biomass

We estimated biovolume (determined from area-by-diameter estimation) and cell density using a FlowCAM (VS Series, Fluid Imaging Technologies, Scarborough, MA) at a flow rate of 0.3 mL/min. We converted biovolume to biomass, M_i (μg C = $0.109(\text{biovolume})^{0.991}$; Montagnes et al. 1994; appendix; supplementary methods, figs. A2, A3; appendix is available online).

Estimating the Temperature Dependence of Photosynthesis and Respiration

We determined the activation energy of photosynthesis and respiration over a temperature range from 8° to 24°C by measuring oxygen production in the light and oxygen consumption in the dark using a 24-channel optical fluorescence oxygen system (Sensor Dish Reader SDR2, PreSens), equipped with a 24-chamber 200-μL glass microplate (Loligo Systems Aps, Tjele, Denmark). The oxygen sensor was placed in a temperature-controlled incubator (Panasonic M1R-154) with light at 80 μmol/m^2/s. Prior to measurements of net photosynthesis and respiration, 200 μL of well-mixed *T. tetrahele* cultures at densities of ~20,000 cells/mL, equivalent to carrying capacity at 16°C, were transferred from 30-mL test tubes to each microplate well. Wells were sealed with transparent polymerase chain reaction film (Thermo Scientific, Waltham, MA), and measurements of oxygen concentrations were taken every 15 s over 3-h periods, first in darkness and next in light, using the SDR v4.0 software (PreSens, Germany). Prior to oxygen flux measurements, sensor spots were calibrated with air-saturated water and water containing 2% sodium sulfite at each experimental temperature. After a 4-h gradual increase or decrease from 16°C to each assay temperature, phytoplankton cells were acclimated for an hour in the dark prior to measurements.

We estimated gross photosynthesis as GP = NP + R at each temperature, where NP is net oxygen production rate (NP, mg O_2 mL^{-1} h^{-1}) and R is respiration rate, or net oxygen consumption rate (R, mg O_2 mL^{-1} h^{-1}). We measured rates on each plankton sample in dark and light conditions and then estimated GP for each sample (n = 18 at each test temperature). We corrected for background microbial activity by subtracting from each respiration estimate the average oxygen flux from six control wells containing ESAW medium but no phytoplankton. We estimated per capita mass-normalized metabolic rates (B_i) by dividing oxygen fluxes by total population biomass estimated immediately before respirometry experiments. We used ordinary least squares (OLS) regression to estimate activation energies (E; eq. [3]) from relationships between log-transformed mass-normalized oxygen flux rates and temperature (1/kT).

Estimating the Temperature Dependence of Carrying Capacity and Cell Size

We initiated five replicate experimental populations of *T. tetrahele* in 30-mL glass test tubes containing 25 mL of 10 μM nitrate ESAW medium at a density of 1,000 cells/mL at 5°, 8°, 16°, 25°, 32°, and 38°C. Experimental populations were held at constant temperature and light conditions (16L : 8D photoperiod; 60 μmol/m^2/s) until they reached steady state at all temperatures. We measured cell densities (cells/mL) and biovolumes (μm^3/cell/mL) from 250-μL samples every 4 days at the same time of day for 43 days until populations at all temperatures had reached carrying capacity (i.e., steady state; fig. A4).

To test our hypotheses (eq. [7]), we estimated K in terms of density (K_N, individual cells/mL, consistent with eq. [2]) and in terms of population biomass (K_{Bio}). To estimate K_N, we fit a logistic growth model (eq. [1]) to population abundance time series data using nonlinear regression with the nlsLM function in R, which uses the Levenberg-Marquart optimization algorithm in the minpack.LM package (ver. 1.2.1; Elzhov et al. 2016). We used the nls.multstart package (ver. 1.0.0; Padfield and Matheson 2018) to iterate more than 1,000 different combinations of starting values drawn from a uniform distribution and chose the best model selected via the lowest Akaike information criterion score. We quantified model fits graphically and by calculating Efron's pseudo-R^2 values (noting that R^2 values are often a poor indicator of the performance of a nonlinear model and require a different interpretation than for linear models; Spiess and Neumeyer 2010). We estimated uncertainty in model fits by bootstrap resampling the original time series data, refitting the logistic model 1,000 times and plotting 95% confidence intervals (CI; figs. A4, A5). To estimate K_{Bio}, we fit the logistic model to time series of population biomass. We estimated the fractional decrease in body size with each degree increase in temperature, β, with OLS regression, using average cell size in each population at carrying capacity, and set T_{R} at 5°C, the coldest temperature in our experiment. We used OLS regression to estimate the temperature dependence of mass-normalized carrying capacity $\ln(K_N M_i(T)^{3/4})$ and $\ln(K_{\text{Bio}})$. We conducted all statistical analyses in R (ver. 3.4.1; R Development Core Team 2017) and used the purrr (ver. 0.2.3; Henry and Wickham 2017), broom (ver. 0.4.2; Robinson 2017), and modelr (ver. 0.1.1; Wickham 2017) packages to facilitate data manipulation and analysis. All data are deposited in the Dryad Digital Repository: https://doi.org/10.5061/dryad.9kv23s3 (Bernhardt et al. 2018).

Results

Temperature Dependence of Photosynthesis and Respiration

The activation energies of mass-normalized oxygen fluxes in *Tetraselmis tetrahele* were E_{NP} = 0.24 eV (95% CI: −0.02, 0.51; table 1) for net photosynthesis, E_R = 0.52 eV (95% CI: 0.39, 0.66; table 1) for respiration, and E_{GP} = 0.33 eV (95% CI: 0.20, 0.46; table 1) for gross photosynthesis (fig. 1). The ratio of the two fluxes, ln(GP/R), decreased with increasing temperature with a temperature dependence of $E_{\text{GP}/R}$ = −0.20 eV (95% CI: −0.32, −0.08; table 1; fig. A6).

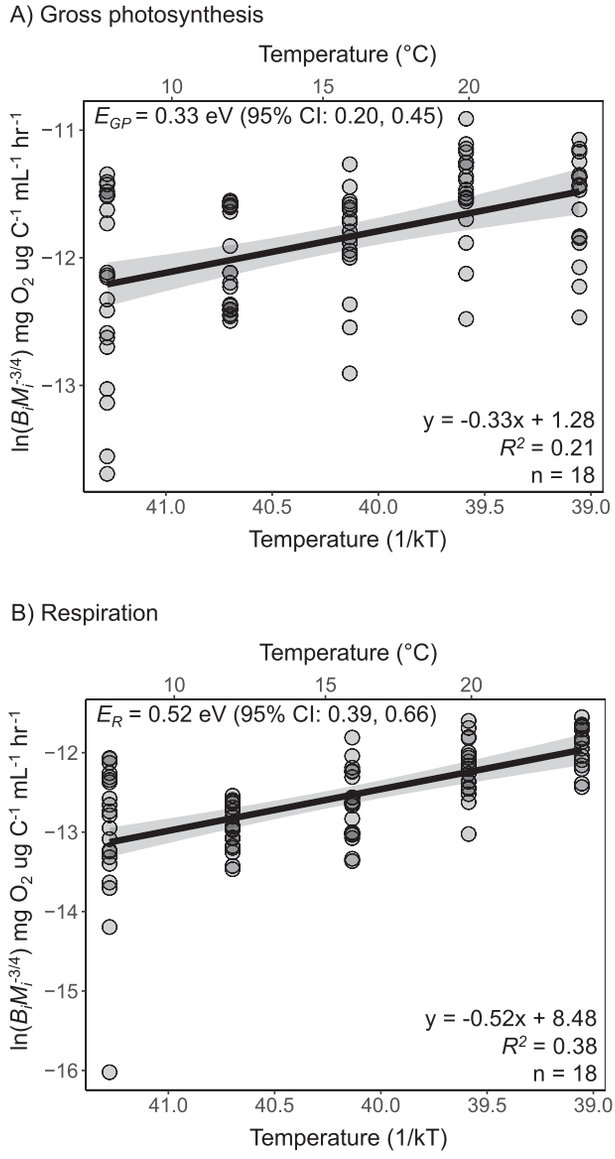

Figure 1: Mass-normalized metabolic rates ($B_i M_i^{-3/4}$) of *Tetraselmis tetrahele* increased with temperature for gross photosynthesis (*A*) and for respiration ($n = 18$ per test temperature; *B*). Points are shown at medium opacity to indicate overlap; shaded bands refer to 95% confidence intervals from ordinary least squares regression. For ease of interpretation, a secondary horizontal axis (upper axis) shows temperature in degrees Celsius.

Temperature Dependence of Cell Size and Carrying Capacity

Population density and cell size at carrying capacity decreased with increasing temperature (figs. 2, 3). Cell size decreased by 1.92% per degree increase in temperature (−1.57 μg C/°C; 95% CI: −1.94, −1.21; adjusted $R^2 = 0.81$, corresponding to a fractional decrease in body size, $\beta = 1.92\%\ °C^{-1}$; table 1; fig. 3*A*). This change was detected as early as day 4 in the experiment and persisted until steady state (fig. A7).

Mass-normalized density at steady state, $\ln(K_N M_i(T)^{3/4})$, decreased with increasing temperature with a temperature dependence of $E_{K,N} = -0.22$ eV (95% CI: −0.25, −0.18; table 1), less than our prediction from our first hypothesis that $E_{K,N} = -E_{GP} = -0.33$ eV (eq. [7]; $\beta = 0$; fig. 2*A*). When we used equation (7) to predict density at steady state, $\ln(K_N M_i(T)^{3/4})$, using $\beta = 1.92\%°C^{-1}$ and $E_{GP} = 0.33$ eV (fig. 1), we predicted a density decline with increasing temperature $E_{K,N} = -0.21$ eV (fig. 2*A*). This prediction is statistically indistinguishable from the empirical estimate of the temperature dependence of $\ln(K_N M_i^{3/4})$ (fig. 2*A*). This result did not change when we used the observed average cell size in each population at carrying capacity in the mass normalization of K_N, $K_N M_i(T)^{3/4}$, and thus the observed activation energy was $E_{K,N} = -0.34$ eV (95% CI: −0.31, −0.37), which is statistically indistinguishable from the prediction that $E_{K,N} = -E_{GP} = -0.33$ eV (fig. 2*B*).

We also estimated carrying capacity from time series of population biomass, which combines cell size and cell number. The $\ln(K_{Bio})$ decreased with increasing temperature with a slope of $E_{K,Bio} = -0.30$ eV (95% CI: −0.33, −0.26; table 1; fig. 3*B*), which is statistically indistinguishable from the predicted slope of −0.33 eV. Population-level nitrate used at steady state, estimated as nitrate remaining in the microcosms, did not change with temperature (OLS regression slope = 0.055, 95% CI: −0.29, 0.19; fig. 3*C*).

Including data from the warmer-than-optimal 32°C populations in the activation energy estimation for K_N and K_{Bio} introduced a nonlinear decline in $\ln(K)$ such that abundance declined much more rapidly above 25°C (fig. A8); therefore, these populations were not included in the linear fits (figs. 2, 3). We observed no population growth at 38°C and did not estimate K for these populations. These abundance declines are consistent with dominance of physiological stress responses to temperature as it rises past the thermal optimum in *T. tetrahele*, which is ~25°C (fig. A1).

Discussion

Consistent with the metabolic theory of ecology that links general trends in individual metabolic rate to macroecological patterns in population and ecosystem patterns (Enquist et al. 2003; Brown et al. 2004; Savage et al. 2004), we found that carrying capacity varies with the temperature dependence of photosynthesis and the temperature dependence of body size in a model species, the chlorophyte *Tetraselmis tetrahele*. While K declined with warming, the concomitant reduction in body size of approximately $\beta = 1.92\%°C^{-1}$ meant that K did not decline by nearly as much as would have been predicted by MTE when assuming a temperature-invariant body size. Our results provide empirical support for the often-

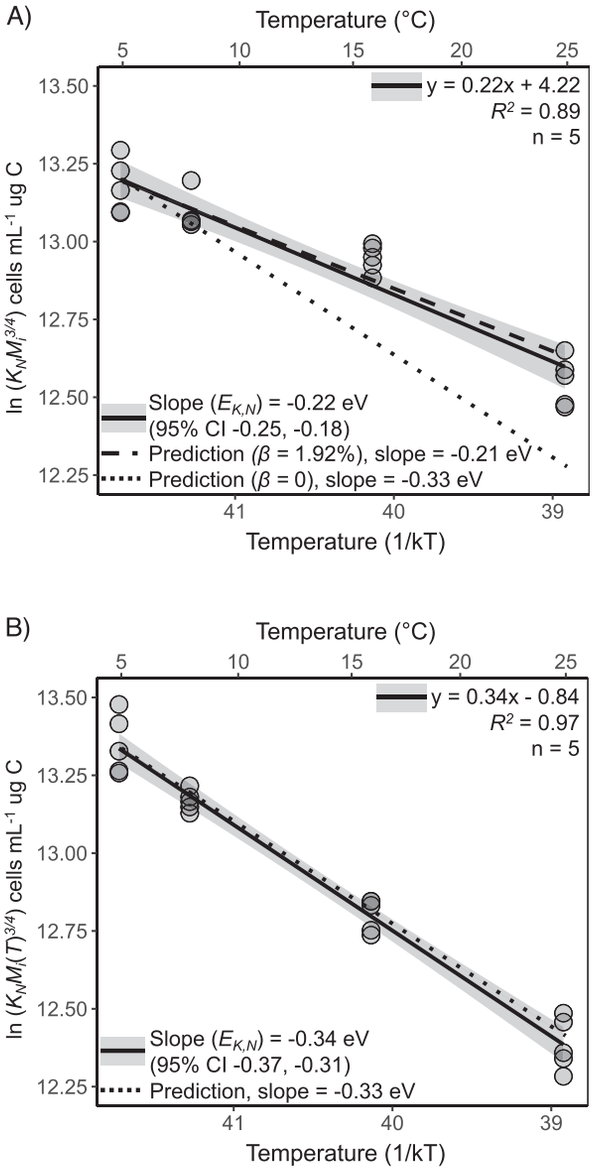

Figure 2: Carrying capacity declined as temperature increased. *A*, Mass-normalized carrying capacity (cells mL^{-1} μg C), $K_N M_i^{3/4}$, decreased with increased temperature ($n = 5$ per test temperature). Ordinary least squares (OLS) regression of observed density over the temperature gradient (solid line; shaded area represents 95% confidence intervals) diverged from the model prediction (dotted line) based on equation (7) assuming temperature-independent body mass ($\beta = 0$). The model prediction based on equation (7) that included the observed decline in body size with increasing temperature ($\beta = 1.92\%$ °C^{-1}; thick dashed line) matched OLS regression to observed results. *B*, Mass-normalized carrying capacity (cells mL^{-1} μg C), $K_N M_i(T)^{3/4}$, decreased with temperature; M_i varied with temperature and corresponds to the average cell biomass in each replicate population at carrying capacity. For ease of interpretation, a secondary horizontal axis (upper axis) shows temperature in degrees centigrade.

assumed negative relationship between carrying capacity and temperature mediated by increased per capita metabolic rates (O'Connor et al. 2011; Rall et al. 2012; Gilbert et al. 2014) but also demonstrate that when linking metabolic rates to population dynamics, effects of temperature on body size cannot be ignored.

We empirically estimated an activation energy of $E_{GP} = 0.33$ eV for gross photosynthesis, consistent with previously published estimates of the activation energy of photosynthesis in phytoplankton (Allen et al. 2005; López-Urrutia et al. 2006; Regaudie-De-Gioux and Duarte 2012; Yvon-Durocher and Allen 2012). Recent studies have found that the temperature dependence of gross photosynthesis in phytoplankton constrains outcomes of population-level ecological and evolutionary processes (Padfield et al. 2016; Schaum et al. 2017). In our study, this temperature dependence predicted the general decline in total biomass with warming, but quantitatively, our observed population densities at warmer temperatures were higher than expected based on the temperature dependence of photosynthesis alone. However, when we considered the phenotypic decline in body size at warmer temperatures and the expectation that smaller body sizes could allow greater density per unit population biomass, we were able to accurately predict density declines at higher temperatures. This suggests that a phenotypic change in body size, consistent with the widely observed temperature-size rule, was associated with lower per capita resource use that may have mitigated the effect of increased metabolic rates on density but not total biomass. Our finding that using a linear approximation of the temperature-size rule (captured by β) accurately predicts declines in abundance with temperature suggests that in the absence of estimates of body size for all individuals in the population, a general relationship between size and temperature for a system may provide a reasonable estimate of the indirect effects of temperature-dependent body size on carrying capacity. Other undetected phenotypic changes may have occurred during the course of the experiment, which could also change the relationship between instantaneous metabolic demand and carrying capacity. Nevertheless, the link between temperature, metabolic rate, and carrying capacity we present here provides a mechanistic lens for understanding previous studies that have reported similar negative temperature dependence of carrying capacity and assumed, rather than measured, metabolic rates (Alto and Juliano 2001; West and Post 2016).

Divergent responses of population density and population biomass to temperature have implications for higher-order processes in ecosystems. While total biomass is often considered an important estimate of ecosystem functions, the number and size of individuals influence demographic processes and their outcomes. Theoretical analyses that have extended the metabolic theory of ecology to population dynamics in consumer-resource systems have shown that the temperature-

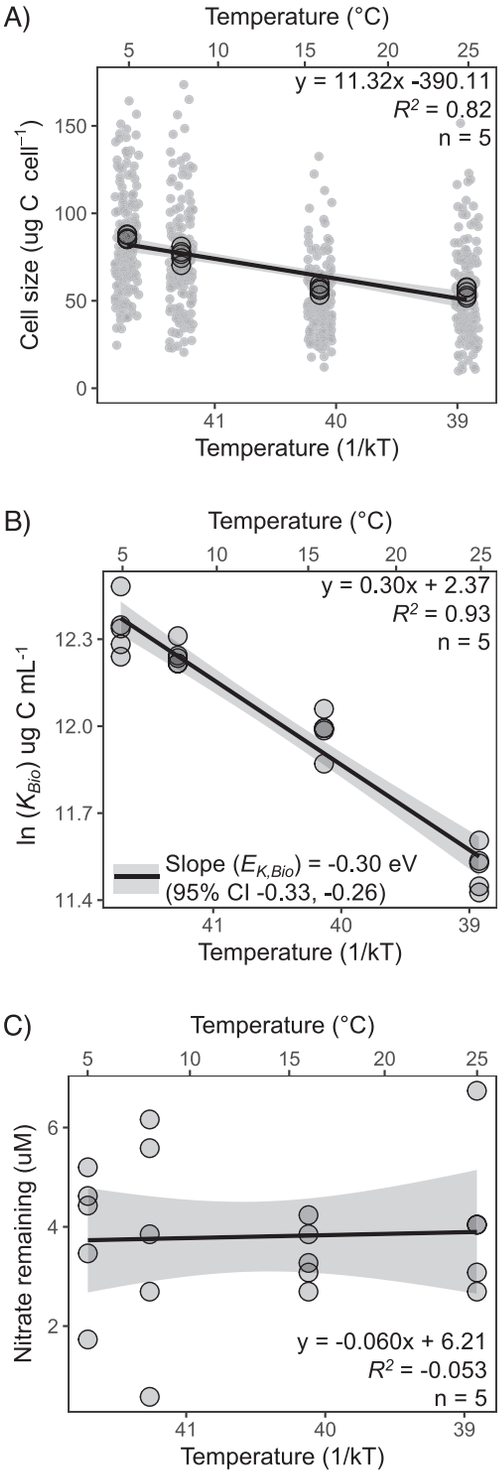

Figure 3: Cell size (μg C cell^{-1}; *A*), estimated population biomass ln (K_{Bio}) (μg C mL^{-1}; *B*), and nitrate remaining in microcosms (*C*) at carrying capacity across a temperature gradient from 5° to 25°C (shaded bands in all panels represent 95% confidence intervals from ordinary least squares regression [OLS]). *A*, Observed cell sizes are shown (large circles represent population mean cell size, $n = 5$ populations per test temperature, and small gray dots represent individual cell size estimates, subsample of $n = 30$ per population, pooled across populations to show the spread in cell size, with OLS regression fit to population-level data). For ease of interpretation, a secondary horizontal axis (upper axis) shows temperature in degrees centigrade.

size rule can stabilize consumer-resource systems over temperature gradients (Osmond et al. 2017). The effects of smaller body size on population growth rate and consumer-resource interactions counteract the expected effects of temperature on growth rates and carrying capacity, thereby allowing greater persistence of systems in warming environments compared to systems in which body size does not change with temperature (Osmond et al. 2017; Sentis et al. 2017; Uszko et al. 2017). The dynamical consequences of body-size shifts are an important link between organismal responses to temperature and ecosystem-level patterns of diversity and energy flux. This stabilizing effect of the temperature-size rule on dynamics suggests that as per capita metabolic rates increase with warming, population collapses that might be expected due to destabilizing dynamics do not occur.

Relating our findings to other reports from laboratory and field assessments of population abundance as a function of temperature is not straightforward without clear evidence that observations met the conditions assumed by equation (7), namely, that resource supply remained constant across temperature treatments, the temperature dependence of the metabolic rate most relevant to limiting growth is known, and body size did not change with temperature. Some studies in microbial systems have reported weak or no response of carrying capacity to temperature (Zwietering et al. 1991; Urit et al. 2013; Arandia-Gorostidi et al. 2017). The ability of bacteria in anaerobic systems to maintain density over a thermal gradient may reflect their use of multiple metabolic pathways, each with a distinct temperature dependence—not the highly conserved photosynthesis and aerobic respiration used by most phytoplankton. Further, these studies report only cell density and do not provide observations of metabolic rate or cell size over the thermal gradient, so they do not provide data sufficient to test hypotheses derived from equation (7). Other studies report increasing, decreasing, or unimodal changes in abundance correlated with temperature under conditions in which resource supply was not controlled (Meehan 2006; Isaac et al. 2011; O'Gorman et al. 2017) or was controlled but unknown (Fox and Morin 2001; Jiang and Morin 2004).

The relationship between density at equilibrium and temperature hinges on how per capita resource demand varies with temperature. Models of algal growth have described per capita resource demand as increasing, decreasing, or independent of temperature (Tilman et al. 1981; Toseland et al. 2013; Daines et al. 2014; Thomas et al. 2017; Uszko et al. 2017). Consistent with the predictions of MTE (Savage et al. 2004), our

findings suggest that per capita resource demand increased in warm conditions, and nutrient use efficiency increased at larger cell sizes and colder conditions. Given the same supply of resources (P) to all populations across our experimental temperature gradient, increasing temperatures resulted in lower population abundances, in which each individual was fluxing energy and materials at higher rates. We observed that population-level resource use (measured as nitrate remaining in the microcosms at steady state) was the same across all temperatures, despite higher population abundances and larger cell sizes in the cold, suggesting that warm populations had higher per capita resource demands. This suggests that under cold conditions, *T. tetrahele* is more efficient at converting the limiting nutrient into biomass (Marañón et al. 2013, 2018). This greater efficiency is also consistent with the temperature dependence of the ratio of GP/R (fig. A6), which suggests that at colder temperatures, a smaller fraction of carbon fixed is respired immediately. Models of temperature-dependent resource allocation support this finding: as temperatures increase, phytoplankton are predicted to decrease investment in phosphorus-rich ribosomes and increase investment in nitrogen-rich light-harvesting machinery, leading to higher per capita nitrogen demand (Toseland et al. 2013). In addition to the direct effects of temperature on per capita resource use, temperature may also affect per capita resource use indirectly via shifts in cell size. In marine phytoplankton, maximum nutrient uptake rates increase isometrically with cell size (Marañón et al. 2013), while minimum nitrogen requirements scale with negative allometry (i.e., scale with a slope of ~0.87), meaning that larger cells are more mass efficient at converting nutrients to biomass (Marañón et al. 2013).

Here we showed that carrying capacity of photosynthetic autotrophs declined with increasing temperature as simple functions of the increase in per capita gross photosynthetic rate and temperature-driven decline in body size. We extended metabolic theory models to include predictions that account for concomitant changes in body size with temperature described by the temperature-size rule. This work bolsters a key assumption in the metabolic scaling framework for how the temperature dependence of subcellular processes influences ecosystem processes, via population dynamics. Our empirical system was intentionally simple and designed to meet the assumptions of a simple population model. The link between per capita metabolic rates and demographic outcomes will likely be more complex when multiple species or longer temporal dynamics are examined. For example, changes in allocation of resources to reproduction, varying resource dynamics, or evolution may alter the relationship between instantaneous metabolic rates and demographic processes (Michaletz et al. 2014; Padfield et al. 2016; Osmond et al. 2017; Uszko et al. 2017; Kirk et al. 2018). As the metabolic theory of ecology continues to expand and incorporate additional complexity and ecological processes, such complexities can be modeled and understood in relation to the simpler dynamics we have demonstrated here. In this way, the metabolic theory of ecology serves as a framework to unite dynamical models and empirical evidence for ecological responses to temperature, from organisms to ecosystems.

Acknowledgments

We thank E. Yangel for help with data collection and the O'Connor Lab for many useful discussions about carrying capacity. Funding was provided by a Vanier Canada Graduate Scholarship (J.R.B.), the Biodiversity Research Centre (J.M.S.), and the Natural Sciences and Engineering Research Council (M.I.O.).

Literature Cited

Allen, A. P., J. F. Gillooly, and J. H. Brown. 2005. Linking the global carbon cycle to individual metabolism. Functional Ecology 19:202–213.

———. 2007. Recasting the species-energy hypothesis: the different roles of kinetic and potential energy in regulating biodiversity. Pages 283–299 *in* D. Storch, P. Marquet, and J. Brown, eds. Scaling biodiversity. Cambridge University Press, Cambridge.

Alto, B. W., and S. A. Juliano. 2001. Temperature effects on the dynamics of *Aedes albopictus* (Diptera: Culicidae) populations in the laboratory. Journal of Medical Entomology 38:548–556.

Anderson-Teixeira, K. J., P. M. Vitousek, and J. H. Brown. 2008. Amplified temperature dependence in ecosystems developing on the lava flows of Mauna Loa, Hawai'i. Proceedings of the National Academy of Sciences of the USA 105:228–233.

Arandia-Gorostidi, N., T. M. Huete-Stauffer, L. Alonso-Sáez, and X. A. G. Morán. 2017. Testing the metabolic theory of ecology with marine bacteria: different temperature sensitivity of major phylogenetic groups during the spring phytoplankton bloom. Environmental Microbiology 19:4493–4505.

Atkinson, D., B. J. Ciotti, and D. J. S. Montagnes. 2003. Protists decrease in size linearly with temperature: ca. 2.5% $°C^{-1}$. Proceedings of the Royal Society B 270:2605–2611.

Bernhardt, J. R., J. M. Sunday, and M. I. O'Connor. 2018. Data from: Metabolic theory and the temperature size rule explain the temperature dependence of population carrying capacity. American Naturalist, Dryad Digital Repository, https://doi.org/10.5061/dryad.9kv23s3.

Bolker, B. 2017. bbmle: tools for general maximum likelihood estimation. https://rdrr.io/cran/bbmle/.

Brown, J. H., J. F. Gillooly, A. P. Allen, V. M. Savage, and G. B. West. 2004. Toward a metabolic theory of ecology. Ecology 85:1771–1789.

Daines, S. J., J. R. Clark, and T. M. Lenton. 2014. Multiple environmental controls on phytoplankton growth strategies determine adaptive responses of the N:P ratio. Ecology Letters 17:414–425.

Damuth, J. 1987. Interspecific allometry of population density in mammals and other animals: the independence of body mass and population energy-use. Biological Journal of the Linnean Society 31:193–246.

DeLong, J. P. 2012. Experimental demonstration of a "rate-size" tradeoff governing body size optimization. Evolutionary Ecology Research 14:343–352.

Doebeli, M., Y. Ispolatov, and B. Simon. 2017. Towards a mechanistic foundation of evolutionary theory. eLife 6:e23804.

Elzhov, T. V., K. M. Mullen, A.-N. Spiess, and B. Bolker. 2016. minpack.lm: R interface to the Levenberg-Marquardt nonlinear least-squares algrothim found in MINPACK, plus support for bounds. R package, version 1.2-1. https://cran.rproject.org/web/packages/minpack.lm/minpack.lm.pdf.

Enquist, B. J., E. P. Economo, T. E. Huxman, A. P. Allen, D. D. Ignace, and J. F. Gillooly. 2003. Scaling metabolism from organisms to ecosystems. Nature 423:639–642.

Eppley, R. W. 1972. Temperature and phytoplankton growth in the sea. Fishery Bulletin 70:1063–1085.

Forster, J., A. G. Hirst, and D. Atkinson. 2012. Warming-induced reductions in body size are greater in aquatic than terrestrial species. Proceedings of the National Academy of Sciences of the USA 109: 19310–19314.

Fox, J. W., and P. J. Morin. 2001. Effects of intra- and interspecific interactions on species responses to environmental change. Journal of Animal Ecology 70:80–90.

Fronhofer, E. A., and F. Altermatt. 2015. Eco-evolutionary feedbacks during experimental range expansions. Nature Communications 6:6844.

Gilbert, B., T. D. Tunney, K. S. Mccann, J. P. Delong, D. A. Vasseur, V. Savage, J. B. Shurin, et al. 2014. A bioenergetic framework for the temperature dependence of trophic interactions. Ecology Letters 17:902–914.

Gillooly, J. F., J. H. Brown, G. B. West, V. M. Savage, and E. L. Charnov. 2001. Effects of size and temperature on metabolic rate. Science 293:2248–2251.

Gotelli, N. J. 1995. A primer of ecology. Sinauer, Sunderland, MA.

Harrison, P. J., R. E. Waters, and F. J. R. Taylor. 1980. A broad spectrum artificial sea water medium for coastal and open ocean phytoplankton. Journal of Phycology 16:28–35.

Hendry, A. 2017. Eco-evolutionary dynamics. Princeton University Press, Princeton, NJ.

Henry, L., and H. Wickham. 2017. purrr: functional programming tools. https://purrr.tidyverse.org/.

Isaac, N. J. B., M. Girardello, T. M. Brereton, and D. B. Roy. 2011. Butterfly abundance in a warming climate: patterns in space and time are not congruent. Journal of Insect Conservation 15:233–240.

Jiang, L., and P. J. Morin. 2004. Temperature-dependent interactions explain unexpected responses to environmental warming in communities of competitors. Journal of Animal Ecology 73:569–576.

Kirk, D., N. Jones, S. Peacock, J. Phillips, P. K. Molnár, M. Krkošek, and P. Luijckx. 2018. Empirical evidence that metabolic theory describes the temperature dependency of within-host parasite dynamics. PLoS Biology 16:e2004608.

Kremer, C. T., M. K. Thomas, and E. Litchman. 2017. Temperature- and size-scaling of phytoplankton population growth rates: reconciling the Eppley curve and the metabolic theory of ecology. Limnology and Oceanography 62:1658–1670.

López-Urrutia, Á. 2008. The metabolic theory of ecology and algal bloom formation. Limnology and Oceanography 53:2046–2047.

López-Urrutia, A., E. San Martin, R. P. Harris, and X. Irigoien. 2006. Scaling the metabolic balance of the oceans. Proceedings of the National Academy of Sciences of the USA 103:8739–8744.

Mallet, J. 2012. The struggle for existence: how the notion of carrying capacity, *K*, obscures the links between demography, Darwinian evolution, and speciation. Evolutionary Ecology Research 14:627–665.

Marañón, E., P. Cermeño, D. C. López-Sandoval, T. Rodríguez-Ramos, C. Sobrino, M. Huete-Ortega, J. M. Blanco, and J. Rodríguez. 2013. Unimodal size scaling of phytoplankton growth and the size dependence of nutrient uptake and use. Ecology Letters 16:371–379.

Marañón, E., M. P. Lorenzo, P. Cermeño, and B. Mouriño-Carballido. 2018. Nutrient limitation suppresses the temperature dependence of phytoplankton metabolic rates. ISME Journal 12:1836–1845.

McCann, K. S. 2011. Food webs. Princeton University Press, Princeton, NJ.

Meehan, T. D. 2006. Energy use and animal abundance in litter and soil communities. Ecology 87:1650–1658.

Michaletz, S. T., D. Cheng, A. J. Kerkhoff, and B. J. Enquist. 2014. Convergence of terrestrial plant production across global climate gradients. Nature 512:39–43.

Montagnes, D. J. S., J. A. Berges, P. J. Harrison, and F. J. R. Taylor. 1994. Estimating carbon, nitrogen, protein, and chlorophyll *a* from volume in marine phytoplankton. Limnology and Oceanography 39:1044–1060.

O'Connor, M. I., B. Gilbert, and C. J. Brown. 2011. Theoretical predictions for how temperature affects the dynamics of interacting herbivores and plants. American Naturalist 178:626–638.

O'Gorman, E. J., L. Zhao, D. E. Pichler, G. Adams, N. Friberg, B. C. Rall, A. Seeney, H. Zhang, D. C. Reuman, and G. Woodward. 2017. Unexpected changes in community size structure in a natural warming experiment. Nature Climate Change 7:659–663.

Osmond, M. M., M. A. Barbour, J. R. Bernhardt, M. W. Pennell, J. M. Sunday, and M. I. O'Connor. 2017. Warming-induced changes to body size stabilize consumer-resource dynamics. American Naturalist 189:718–725.

Padfield, D., C. Lowe, A. Buckling, R. Ffrench-Constant, Student Research Team, S. Jennings, F. Shelley, J. S. Ólafsson, and G. Yvon-Durocher. 2017. Metabolic compensation constrains the temperature dependence of gross primary production. Ecology Letters 20:1250–1260.

Padfield, D., and G. Matheson. 2018. nls.multstart. https://cran.r-project.org/web/packages/nls.multstart/index.html.

Padfield, D., G. Yvon-Durocher, A. Buckling, S. Jennings, and G. Yvon-Durocher. 2016. Rapid evolution of metabolic traits explains thermal adaptation in phytoplankton. Ecology Letters 19:133–142.

Pauly, D., and V. Christensen. 1995. Primary production required to sustain global fisheries. Nature 374:255–257.

Pawar, S., A. I. Dell, V. M. Savage, J. L. Knies, M. Kearney, and S. Kalisz. 2016. Real versus artificial variation in the thermal sensitivity of biological traits. American Naturalist 187:E41–E52.

Pena, M. R., and C. T. Villegas. 2005. Cell growth, effect of filtrate and nutritive value of the tropical Prasinophyte *Tetraselmis tetrathele* (Butcher) at different phases of culture. Aquaculture Research 36: 1500–1508.

Rall, B. C., U. Brose, M. Hartvig, G. Kalinkat, F. Schwarzmüller, O. Vucic-Pestic, and O. L. Petchey. 2012. Universal temperature and body-mass scaling of feeding rates. Philosophical Transactions of the Royal Society B 367:2923–2934.

R Development Core Team. 2017. R: a language and environment for statistical computing. R Foundation for Statistical Computing, Vienna.

Regaudie-De-Gioux, A., and C. M. Duarte. 2012. Temperature dependence of planktonic metabolism in the ocean. Global Biogeochemical Cycles 26, doi:10.1029/2010GB003907.

Robinson, D. 2017. broom: convert statistical analysis objects into tidy data frames. https://rdrr.io/cran/broom/man/broom.html.

Sarker, S., and K. H. Wiltshire. 2017. Phytoplankton carrying capacity: is this a viable concept for coastal seas? Ocean and Coastal Management 148:1–8.

Savage, V. M., J. F. Gillooly, J. H. Brown, G. B. West, and E. L. Charnov. 2004. Effects of body size and temperature on population growth. American Naturalist 163:429–441.

Schaum, C.-E., S. Barton, E. Bestion, A. Buckling, B. Garcia-Carreras, P. Lopez, C. Lowe, et al. 2017. Adaptation of phytoplankton to a decade of experimental warming linked to increased photosynthesis. Nature Ecology and Evolution 1:0094.

Schoolfield, R. M., P. J. H. Sharpe, and C. E. Magnuson. 1981. Nonlinear regression of biological temperature-dependent rate models based on absolute reaction-rate theory. Journal of Theoretical Biology 88:719–731.

Sentis, A., A. Binzer, and D. S. Boukal. 2017. Temperature-size responses alter food chain persistence across environmental gradients. Ecology Letters 20:852–862.

Spiess, A.-N., and N. Neumeyer. 2010. An evaluation of R^2 as an inadequate measure for nonlinear models in pharmacological and biochemical research: a Monte Carlo approach. BMC Pharmacology 10:6.

Strickland, J. D., and T. R. Parsons. 1968. A practical handbook of seawater analysis. Bulletin of the Fisheries Research Board Canada 167:81–86.

Thomas, M. K., M. Aranguren-Gassis, C. T. Kremer, M. R. Gould, K. Anderson, C. A. Klausmeier, and E. Litchman. 2017. Temperature-nutrient interactions exacerbate sensitivity to warming in phytoplankton. Global Change Biology 23:3269–3280.

Tilman, D., M. Mattson, and S. Langer. 1981. Competition and nutrient kinetics along a temperature gradient: an experimental test of a mechanistic approach to niche theory. Limnology and Oceanography 26:1020–1033.

Toseland, A., S. J. Daines, J. R. Clark, A. Kirkham, J. Strauss, C. Uhlig, T. M. Lenton, et al. 2013. The impact of temperature on marine phytoplankton resource allocation and metabolism. Nature Climate Change 3:979–984.

Urit, T., M. Li, T. Bley, and C. Löser. 2013. Growth of *Kluyveromyces marxianus* and formation of ethyl acetate depending on temperature. Applied Microbiology and Biotechnology 97:10359–10371.

Uszko, W., S. Diehl, G. Englund, and P. Amarasekare. 2017. Effects of warming on predator-prey interactions—a resource-based approach and a theoretical synthesis. Ecology Letters 20:513–523.

Vasseur, D. A., and K. S. McCann. 2005. A mechanistic approach for modeling temperature-dependent consumer-resource dynamics. American Naturalist 166:184–198.

Verhulst, P.-F. 1838. Notice sur la loi que la population suit dans son accroissement. Correspondance Mathematique et Physique 10:113–121.

West, D. C., and D. M. Post. 2016. Impacts of warming revealed by linking resource growth rates with consumer functional responses. Journal of Animal Ecology 85:671–680.

Wickham, H. 2017. modelr: modelling functions that work with the pipe. https://modelr.tidyverse.org/.

Yvon-Durocher, G., and A. P. Allen. 2012. Linking community size structure and ecosystem functioning using metabolic theory. Philosophical Transactions of the Royal Society B 367:2998–3007.

Yvon-Durocher, G., J. M. Caffrey, A. Cescatti, M. Dossena, P. Del Giorgio, J. M. Gasol, J. M. Montoya, et al. 2012. Reconciling the temperature dependence of respiration across timescales and ecosystem types. Nature 487:472–476.

Zwietering, M. H., J. T. de Koos, B. E. Hasenack, J. C. de Witt, and K. van't Riet. 1991. Modeling of bacterial growth as a function of temperature. Applied and Environmental Microbiology 57:1094–1101.

References Cited Only in the Online Appendixes

Elzhov, T. V., K. M. Mullen, A.-N. Spiess, and B. Bolker. 2013. minpack.lm: R interface to the Levenberg-Marquardt nonlinear least-squares algorithm found in MINPACK, plus support for bounds. https://cran.r-project.org/web/packages/minpack.lm/index.html.

Marañón, E. 2007. Inter-specific scaling of phytoplankton production and cell size in the field. Journal of Plankton Research 30:157–163.

Menden-Deuer, S., and E. J. Lessard. 2000. Carbon to volume relationships for dinoflagellates, diatoms, and other protist plankton. Limnology and Oceanography 45:569–579.

Reynolds, C. S. 2006. The ecology of phytoplankton. Cambridge University Press, Cambridge.

Thomas, M. K., C. T. Kremer, C. A. Klausmeier, and E. Litchman. 2012. A global pattern of thermal adaptation in marine phytoplankton. Science 338:1085–1088.

Associate Editor: Andrew J. Kerkhoff
Editor: Alice A. Winn

The coastal waters of Vancouver Island, Canada, where the population of the green alga, *Tetraselmis tetrahele*, was collected. Photo credit: Joey Bernhardt.